^1H and ^{13}C Nuclear Magnetic Resonance Studies on Purine

Doris M. Cheng,[1a] Lou S. Kan,[1a] Paul O. P. Ts'o,*[1a] Claude Giessner-Prettre,[1b] and Bernard Pullman[1b]

Contribution from the Division of Biophysics, School of Hygiene and Public Health, The Johns Hopkins University, Baltimore, Maryland 21205, and the Institut de Biologie Physico-Chimique, 75005 Paris, France. *Received March 30, 1979*

Abstract: Both ^1H and ^{13}C resonances of purine have been investigated. In D_2O solution, pH 7.0, 25 °C, the concentration range of purine studied was from 0.001 to 1.04 M for ^1H resonances and 0.02 to 1.01 M for ^{13}C resonances. All ^1H and ^{13}C resonances have been assigned unambiguously together with the determination of all hetero ^{13}C-^1H coupling constants. The magnitudes of these hetero coupling constants are proportional to the electronic density of surrounding atoms. The chemical shifts of the ^1H and ^{13}C resonances of the monomeric, dimeric, and trimeric species of purine in aqueous solutions have been determined with the aid of the knowledge about the mole fractions of these species in solution determined previously from osmotic and activity coefficients. The change of the chemical shifts in the formation of the dimer ($\Delta\delta_2$) and trimer ($\Delta\delta_3$) can then be experimentally measured and compared with the values calculated from the consideration of ring-current magnetic anisotropy as well as local magnetic anisotropy based on the geometry of the stacks. The solvent effect due to the exclusion of water molecules upon stack formation has also been investigated. On the average, the agreement between the experimental and the computed dimerization shifts ($\Delta\delta_2$) for eight resonances has a mean variation of about 0.1 ppm and a standard deviation of 0.2 ppm, and the agreement for the trimerization shifts ($\Delta\delta_3$) has a mean variation of about 0.2 ppm and a standard deviation of 0.3 ppm, with the computed values usually smaller than the observed values. This satisfactory agreement between experimental and computed chemical shifts clearly indicated that the through-space effects of ring current and local magnetic anisotropy can be applied quantitatively to both ^{13}C and ^1H resonances. However, the comparison between the experimental and computed $\Delta\delta_2$ of C_4 and C_5 strongly suggests that there is a shift of population of N_7H tautomers to the N_9H tautomers in the stack, probably owing to a change of dielectric constant from D_2O to the hydrophobic environment of the stack. It should be noted that under certain conditions the solvent effect, i.e., the transfer of nuclei from aqueous environment to hydrophobic environment, on ^{13}C NMR shift, particularly for sp^2 carbon, can be substantial. This effect should be kept in mind in the interpretation of ^{13}C NMR of nucleic acids.

Introduction

Nuclear magnetic resonance spectroscopy has been proven to be one of the most useful techniques in determining molecular conformation in aqueous solution. However, the interpretation of the NMR data, such as chemical shifts and coupling constants, depends on theoretical considerations in order to obtain geometric information about the molecule of interest. For example, the change of the chemical shift of the proton resonances of nucleic acid bases has been explained on the basis of ring-current anisotropy[2] in order to be related to the change of conformation.[3] This approach is semiempirical, and is the same as the Karplus equation which links the dihedral angle to the coupling constants. In order to verify the theory, a quantitative study on a simple model is needed. A verified and perhaps improved theory would increase the accuracy of predictions made for more complicated systems. This strategy has been shown to be successful in ^1H NMR studies on short oligonucleotides.[3]

In recent years, the ^{13}C NMR studies on nucleic acids have blossomed mainly because of improvements in the NMR spectrometer and organic synthesis. However, two basic questions remain unsolved: (1) Can the ring-current anisotropic shielding theory be applied to ^{13}C atoms in nucleic acids? Recently, Vernet and Boekelheide[4] studied ring-current effects on ^{13}C in a substituted purine system and found that shielding effects generally follow the theoretical pattern provided by Johnson and Bovey.[2a] (2) What is the solvent effect on ^{13}C resonances? When two bases are stacked together, certain surrounding water molecules will be excluded. The solvent exclusion effect may be greater on carbon atoms than on protons. In order to answer these two questions, we have chosen to study a simple model, purine. The association of purines in aqueous solution has been well documented.[5-7] The mole fractions of the monomer and associated species of purine in aqueous solution have been evaluated from osmotic and activity coefficients.[5,6] Unequivocal assignments on ^1H resonances of purine have also been made. The thermodynamic data of purine in aqueous solution were analyzed by Cross[8] based on both ^1H and ^{13}C NMR data. The assignment of ^{13}C resonances was first attempted by Pugmire et al.[9] However, the resonances of C_4 and C_5 (see Figure 1) have not been experimentally assigned. The substitution effects on chemical shifts and coupling constants of purine were studied by Thorpe et al.[10] in Me_2SO-d_6. In addition, the tautomeric populations of purine and its derivatives have been studied by Chenon et al.[11] Recently, ^{13}C NMR in configurational assignment of ribofuranosylpurine nucleosides in $CDCl_3$ has been investigated by Fischer et al.[12]

In this paper, we report the experimental assignment of ^{13}C resonances, the concentration dependence of the ^1H and ^{13}C resonances of purine in aqueous solution, as well as the solvent effects of these resonances. An effort was made to interpret these experimental findings based on a quantitative consideration of the combined effects of the ring-current magnetic anisotropy, the local magnetic anisotropy, and the solvent effects on ^1H and ^{13}C resonances.

Experimental and Computational Section

Material. Deuterium oxide (99.8%) was purchased from Bio-Rad Laboratories, Richmond, Calif., and purine was purchased from Sigma Co., St. Louis, Mo. Purine was used without further purification and the samples were lyophilized twice from D_2O. The concentrations of purine solutions were determined by the weight after drying under vacuum. 8-Deuterio- and 6,8-dideuteriopurine were prepared according to the procedures of Schweizer et al.[7] and Pugmire et al.,[9] respectively.

NMR Spectrometry. Both ^1H and ^{13}C NMR spectra of purine and its deuterium analogues were recorded at 99.55 and 25.00 MHz, respectively, using a JEOL FX-100 system operating in the Fourier transform mode. All the spectra were recorded at 25 ± 1 °C, regulated by a JEOL temperature control system, and measured by a United System Corp. 581C digital thermometer.

Chemical-shift data of ^1H and ^{13}C NMR spectra were referred

0002-7863/80/1502-0525$01.00/0

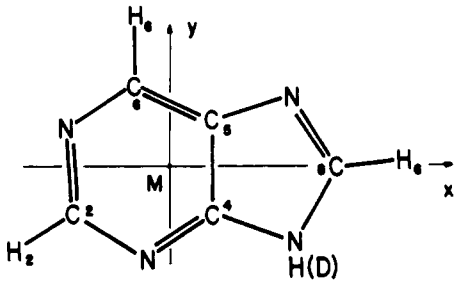

Figure 1. The molecular structure of purine.

respectively to sodium 2,2-dimethyl-2-silapentane-5-sulfonate (DSS) and *p*-dioxane as reference standard by a new procedure. These references (with trace amounts) are not added to the samples; rather they are prepared separately, under identical conditions, i.e., in the same size sample tubes and the same amount of solvent. In utilizing deuterium as a lock signal together with the computer data system, and relying on the precision of the NMR tube, this procedure can produce a reference equivalent to an internal standard. For example, by this procedure the butyl group of *t*-BuOH resonates at 1.237 ppm with respect to the "0" ppm set by DSS. This value is practically the same as that (1.240 ppm) determined in using DSS as an internal standard set at zero position. However, upon the addition of 1.0 M purine, the chemical shift of the butyl group of *t*-BuOH moves upfield to 0.958 ppm, while the internal DSS signal in the purine solution shifts to −0.454 ppm when referenced against external DSS set at 0 ppm. In 1.0 M purine solution the chemical-shift difference between internal DSS and *t*-BuOH is no longer 1.240 ppm, but rather 1.412 ppm. This result indicates that both *t*-BuOH and DSS are shielded to a different extent by purine.[13] By employing the "computer external standard" procedure, it is possible to obtain a reliable reference without having interference or interaction between the sample and the reference. In addition, this method is more accurate than the procedure of inserting a capillary containing the standard into a NMR tube, because not only does the capillary decrease the sensitivity of the sample, but, more importantly, the bulk susceptibility of the reference solution in the capillary is different in the electromagnetic field (sample tube is at *y* axis) and in the superconductive magnetic field (sample tube is at *z* axis).

However, in the study of solvent effects, a concentric, double sample-tube system is employed. For ^{1}H NMR, a capillary containing pure *p*-dioxane as the reference was inserted into a 5-mm tube which contained the compound dissolved in deuterated solvent (for locking purposes) of interest. For ^{13}C NMR, a 8-mm tube containing the compound dissolved in nondeuterated solvent was inserted into a 10-mm tube containing both D_2O (for locking) and *p*-dioxane (for the standard). This arrangement is similar to the procedure used by Mantsch and Smith[14] to study the solvent effect on uridine using ^{13}C NMR.

The calculation of the dimerization and trimerization shifts includes two different contributions: the ring-current effect (RC), which takes into account the large magnetic anisotropy exhibited by the conjugated rings of purine, and the local anisotropy effect (LA), which introduces the anisotropy of the magnetic susceptibility tensors exhibited by the nonhydrogen atoms of the purine molecule at the level of approximation used in the present calculations. The method of computation used in the present work is identical with the one utilized for the determination of the isoshielding curves in ref 15 and is very similar to those of Barfield et al.[16] and Vogler.[17] The ring-current intensities given as input are those of the N_9H tautomer of purine.[18] The atomic magnetic susceptibility tensors are calculated from totally localized orbitals for the σ electrons and from the SCFPPP wave function used in the ring current intensity calculation for the π electrons, according to the formula given previously.[19] The LA effect is calculated within the dipolar approximation since Barfield et al.[16] have clearly shown that the different levels of approximations which can be used for the calculation of the geometrical dependence of the LA effect give equivalent results at intermolecular distances. So the total dimerization shift reported for a given nucleus is

$$\Delta\delta_{2\ \mathrm{total}} = \tfrac{1}{2}(\Delta RC_{12} + \Delta RC_{21}) + \tfrac{1}{2}(\Delta LA_{12} + \Delta LA_{21})$$

where ΔRC_{12} is the ring-current effect of purine 1 on the studied nucleus of purine 2 and ΔRC_{21} is the ring current effect of purine 2 on the same nucleus of purine 1, and where ΔLA_{12} is the local anisotropy effect of all the carbon and nitrogen atoms of purine 1 on the studied nucleus of purine 2 and ΔLA_{21} is the local anisotropy effect of purine 2 on the same nucleus of purine 1. The extension of the above formula to the trimer case is straightforward.

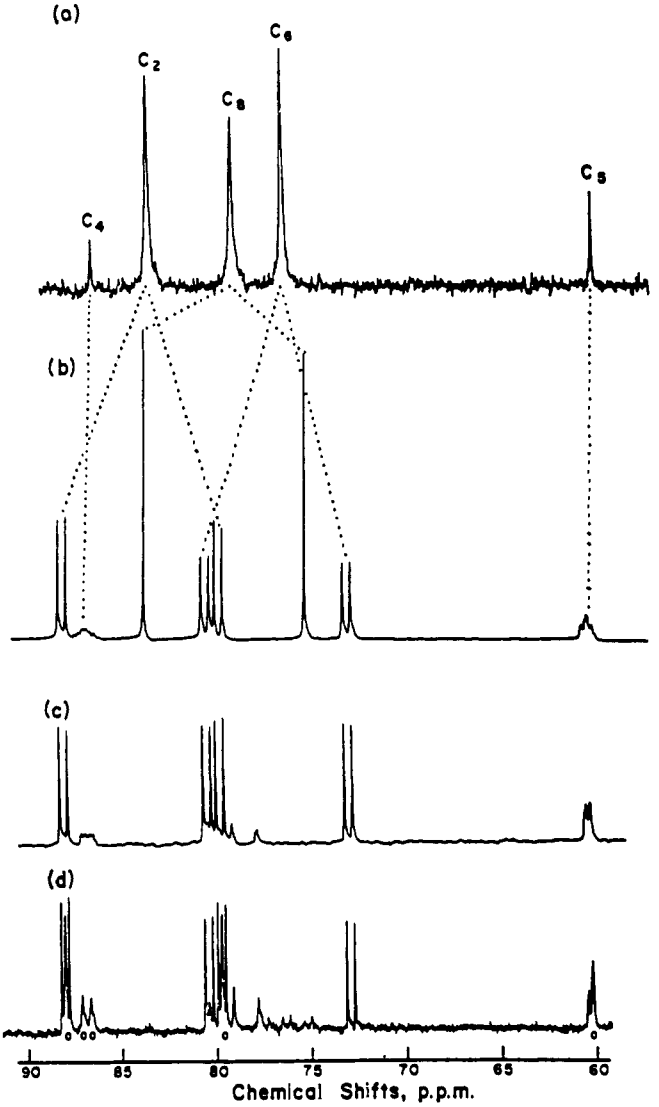

Figure 2. ^{13}C NMR spectra of purine: (a) 1.0 M purine with noise decoupling; (b) 1.0 M purine without noise decoupling; (c) 1.8 M 8-deuteriopurine without noise decoupling; (d) 1.8 M 6,8-dideuteriopurine without noise decoupling. All spectra were recorded at 25 ± 1 °C and the chemical-shift values were measured to *p*-dioxane.

Results

Assignments. Purine has three nonexchangeable protons, i.e., H_2, H_6, and H_8, as shown in Figure 1. The assignment of the resonances of these protons has been well documented in the literature.[7,14] This assignment is reconfirmed by the spectra of deuterium-substituted purines in this work. Purine contains five carbon atoms, C_2, C_4, C_5, C_6, and C_8 (Figure 1). With noise decoupling, five singlets are observed in a ^{13}C NMR spectrum as shown in Figure 2a. The resonances of three carbons, C_2, C_6, and C_8, with directly attached protons, are expected to have shorter relaxation times as compared to those of C_4 and C_5. This is clearly indicated from the intensities of ^{13}C resonances in Figure 2a. Therefore, three signals with relatively high intensity can be readily assigned to C_2, C_6, and C_8, and the remaining two signals with less intensity belong to C_4 and C_5. This gross assignment is further confirmed by the nondecoupling ^{13}C NMR spectrum as shown in Figure 2b.

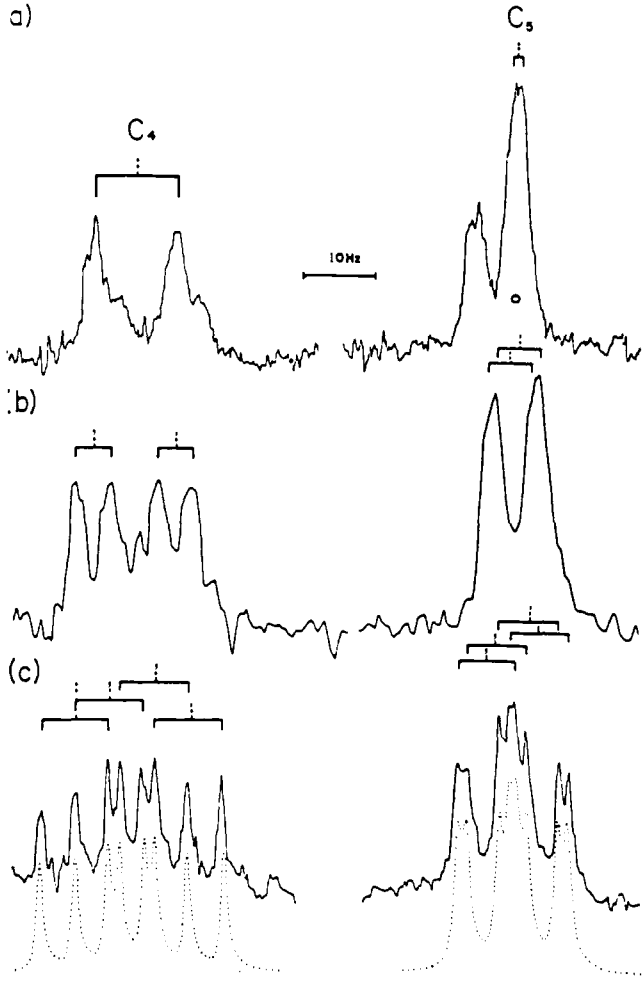

Figure 3. Coupling patterns of C_4 and C_5 resonances of purine. (a) 6,8-Dideuteriopurine, under same experimental condition as Figure 1d. This portion of figure demonstrates the coupling constants of $J_{^{13}C_4-H_2}$ and $J_{^{13}C_5-H_2}$. (b) 8-Deuteriopurine under same experimental conditions as Figure 2c. It demonstrates the coupling constants of $J_{^{13}C_4-H_6}$ and $J_{^{13}C_5-H_6}$. (c) Purine under same experimental conditions as Figure 2b. It demonstrates the coupling constants of $J_{^{13}C_4-H_8}$ and $J_{^{13}C_5-H_8}$. The dotted line is the computer simulation.

Generally, the magnitude of one-bond $^{13}C-H$ coupling is very large, with only the peaks of high intensity showing such splitting and not the lower ones. Therefore, the assignments can be easily grouped into two categories, i.e., C_2, C_6 and C_8 as one category; C_4 and C_5 as the second category. The assignments of the C_2, C_6, and C_8 resonances are first described. Figure 2c shows the ^{13}C NMR spectrum of 8-deuteriopurine without decoupling. One set of doublets disappeared due to the deuterium replacement of hydrogen. Therefore, this doublet or chemical shift at −79.68 ppm must belong to C_8, since one-bond coupling of C_8 to H_8 yields a doublet whereas four-bond C_8 to H_6 coupling yields only a negligible coupling constant. The ^{13}C NMR spectrum of 6,8-dideuteriopurine without proton decoupling is shown in Figure 2d. Only 56% of hydrogen at the C_6 position has been exchanged by deuterium, as shown by integration of ^1H NMR signals of this compound. Therefore, Figure 2d actually shows the ^{13}C NMR spectra of a mixture of 8-deuteriopurine and 6,8-dideuteriopurine. By comparing Figures 2c and 2d, signals with "0" mark are assigned to 6,8-dideuteriopurine and one set of quartets with a chemical shift at −76.80 ppm is assigned to the C_6 resonance. Consequently, the pattern of C_2 resonance should become a doublet due to the expected disappearance of the C_2-H_6 three-bond coupling upon deuterium substitution. In fact, it

Table I. Values of Carbon-Proton Coupling Constants (Hz) of 1.0 M Purine at 25 °C

carbon	proton H_2	proton H_6	proton H_8
C_2	$^1J = 206.5$	$^3J = 10.5$	
C_4	$^3J = 10.8$	$^3J = 4.9$	$^3J = 9.3$
C_5	$^4J = 1.2$	$^2J = 5.9$	$^3J = 8.4$
C_6	$^3J = 10.3$	$^1J = 187.3$	
C_8		$^4J = 0$	$^1J = 212.9$

is shown in Figure 2d since only 56% of H_6 has been deuterated. Therefore, the quartet whose center is −83.96 ppm belongs to C_2. Up to this point, the assignments of C_2, C_6, and C_8 ^{13}C resonances are completed and the results agree with the previous report.[9] Furthermore, the assignments of C_4 and C_5, based on theoretical predictions, can be experimentally verified. Two signals with less intensity of 6,8-dideuteriopurine (with the "0" mark) are enlarged as shown in Figure 3a. Both resonances appear as doublets. However, the one at lower field having a large coupling constant (~10 Hz) and the resonance at higher field having a smaller coupling constant (~1 Hz) are assigned to C_4 and C_5, respectively. This assignment is based on the reasoning that C_4-H_2 is a three-bond coupling whereas C_5-H_2 is a four-bond coupling, and the coupling constant through four covalent bonds is usually smaller in magnitude.[20] The enlarged resonances of C_4 and C_5 of 8-deuteriopurine and purine (Figures 3b and 3c) further support this assignment. The computer-simulated spectrum of C_4 and C_5 resonances in purine is shown as dotted lines in Figure 3. The magnitudes of various types of $^{13}C-H$ hetero couplings are summarized in Table I and the details will be discussed in the next section.

Concentration Dependence. Upon completion of the assignments, chemical shifts of ^1H and ^{13}C resonances of purine are studied from 1.01 to 0.02 M for ^{13}C and 1.04 to 0.001 M for ^1H resonance as shown in Figures 4 and 5. All resonances are shifted upfield as the concentration of purine is increased, with the upfield shift being larger for ^{13}C resonances as compared to ^1H resonances for the same concentration range. The chemical shifts of monomer (δ_1 or the purine at infinite dilutions), dimer (δ_2), and trimer (δ_3) are calculated basically according to the equations by Chan et al.,[21] and are described as follows.

Measurements on ^1H resonances are used as verification of the extrapolation procedure since the data on ^1H can be obtained as low as 0.001 M. The extrapolation procedure proven to be valid experimentally for ^1H resonance is then extended for the analyses of the ^{13}C data. Figures 6–8 demonstrate the extrapolations for obtaining δ_1, δ_2, δ_3 of C_2 and C_5 resonances, respectively. The analyses of the resonance data on these two carbons serve as a representation for the treatment of ^{13}C data on purine based on the equation[21]

$$\delta_{obsd} = \delta_1 F_1 + \delta_2 F_2 + \delta_3(1 - F_1 - F_2) \qquad (1)$$

where δ_{obsd} is the observed chemical shift and F_1, F_2, and F_3 denote respectively the mole fraction of base existing in solution as monomers, dimers, and trimers which were derived from measurements of osmotic and activity coefficients.[5,6] The equilibrium constant used for the calculation of F_1, F_2, and F_3 was verified by three separate measurements and computations over a wide concentration range.[5,6] δ_1 values can be obtained by linear extrapolation of δ_{obsd} to infinite dilution ($F_1 \rightarrow 1$, Figure 6) using the least-squares method. δ_1 of values H_2, H_6, and H_8 are found to be 8.96, 9.15, and 8.60 ppm, respectively, which are in good agreement with the values obtained by extrapolating the concentration-dependent curves shown in Figure 4. The extrapolating procedure based on $(1/\delta_{obsd})/F_1$

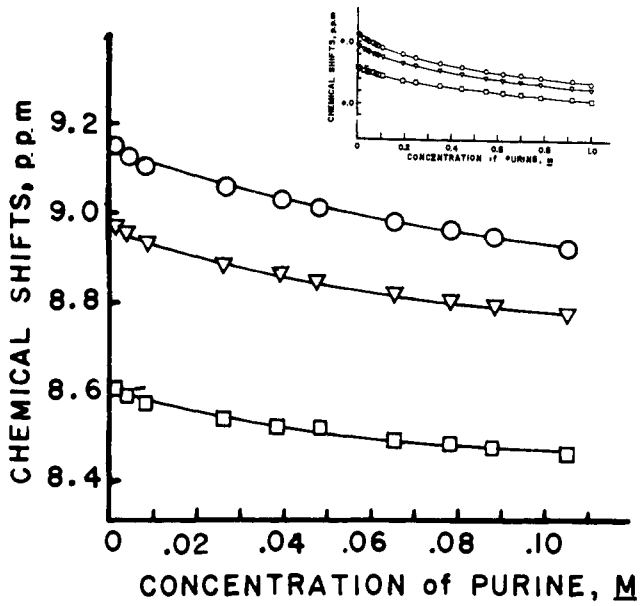

Figure 4. The chemical shifts of ^{1}H NMR of H_2 (▽), H_6 (○), and H_8 (□) resonances vs. the concentration of purine (0.001-1.04 M) at 25 °C. The portion of purine concentration from 0.001 to 0.1 M has been redrawn and enlarged.

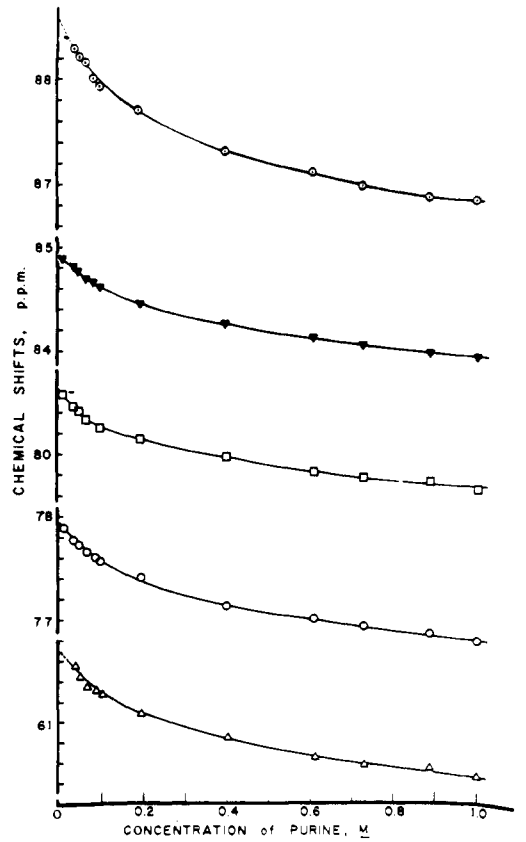

Figure 5. The chemical shifts of ^{13}C NMR of C_2 (▼), C_4 (⊙), C_5 (△), C_6 (○), and C_8 (□) resonances vs. the concentration of purine (0.02-1.01 M) at 25 °C.

vs. m_1 adopted earlier[21] yielded δ_1 values much greater than those obtained from Figure 4. Therefore, the extrapolation procedure shown in Figure 6 is preferred. δ_3 values are obtained by linear plotting of δ_{obsd} vs. $(F_1 + F_2)$ as $(F_1 + F_2)$ approaches zero (Figure 7) with the assumption that $\delta_3 \simeq \delta_4 \simeq \delta_5 \ldots \simeq \delta_\infty$. Again this procedure was found to be more satisfactory than the previous extrapolation procedure using F_1 only.[21]

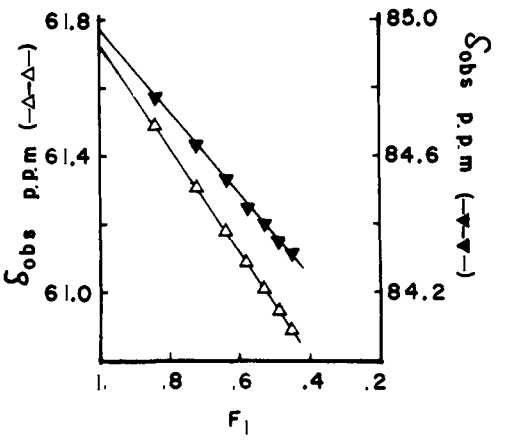

Figure 6. Plot of δ_{obsd} vs. F_1 for obtaining the δ_1 values of C_2 (▼) and C_5 (△) resonances at infinite dilution. Data from Figure 5.

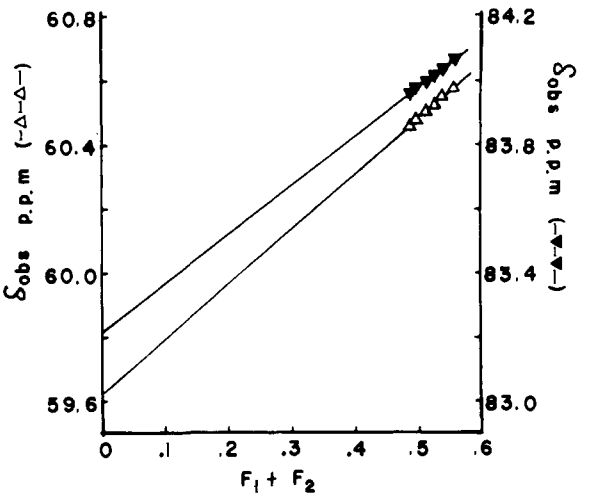

Figure 7. Plot of δ_{obsd} vs. F_1 and F_2 for obtaining δ_3 values of C_2 (▼) and C_5 (△) resonances, at infinite concentration.

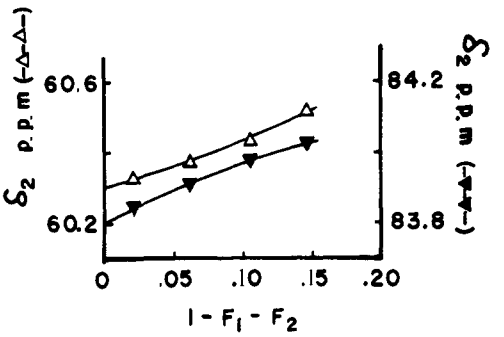

Figure 8. Extrapolation of δ_2 values of C_2 (▼) and C_5 (△) resonances to infinite dilution (see text for δ_2 calculation).

The values of δ_2 are simply calculated from eq 1 at four different concentrations (0.05, 0.10, 0.15, and 0.20 M). Figure 8 shows the extrapolation of δ_2 values from these four concentrations to infinite dilution.

Attempts were made to obtain δ_2 values according to the earlier procedure[21] or the procedure by extrapolating of $(\delta_{obsd} - \delta_1 F_1)/F_2$ as $(1 - F_1 - F_2)$ approaches zero. From the analyses of data on H_2, H_6, and H_8, we find that all extrapolations in the plots are nonlinear as concentration reaches below 0.05 M. Therefore, the approach shown in Figure 8 is adopted instead.

Numerical Analysis. A separate calculation of δ_1, δ_2, and δ_3 has been conducted with the aid of a computer program based

Table II. Values of δ_1, δ_2, and δ_3 of All Proton and Carbon Resonances of Purine in D_2O at 25 °C

	δ values, ppm[a]								
	δ_1			δ_2			δ_3		
		computer regression[c]			computer regression			computer regression	
resonances	graphic extrapolation[b]	full range[d]	low concn range[e]	graphic extrapolation	full range	low concn range	graphic extrapolation	full range	high concn range[f]
C_2	84.97	84.94	84.96	83.83	83.99	83.81	83.21	83.52	83.23
C_4	88.60	88.56	88.62	86.54	86.74	86.44	85.77	86.15	86.04
C_5	61.74	61.68	61.71	60.30	60.40	60.22	59.62	59.95	59.75
C_6	77.98	77.89	77.92	76.67	77.07	76.80	76.06	76.21	76.14
C_8	80.60	80.60	80.64	79.55	79.59	79.26	79.01	79.36	79.05
H_2	8.96	8.94	8.95	8.29	8.50	8.27	7.72	7.87	7.75
H_6	9.15	9.12	9.13	8.38	8.60	8.36	7.69	7.94	7.70
H_8	8.60	8.58	8.59	8.14	8.30	8.07	7.60	7.76	7.54

[a] The standards are DSS and *p*-dioxane for ^1H and ^{13}C NMR measurements, respectively, and all negative signs are omitted. [b] See text and Figures 4, 6, 7, and 8 for the calculations of these values. [c] See text. [d] The concentration ranges for ^1H and ^{13}C NMR data are 0.001-1.04 and 0.02-1.01 M, respectively. [e] The concentration ranges for ^1H and ^{13}C NMR data are 0.001-0.19 and 0.02-0.40 M, respectively. [f] The concentration ranges for ^1H and ^{13}C NMR data are 0.24-1.04 and 0.20-1.01 M, respectively.

Table III. Dimerization Shifts, $\Delta\delta_2$, and Trimerization Shifts, $\Delta\delta_3$, of Purine in D_2O at 25 °C

	exptl $\Delta\delta_2$, ppm		exptl $\Delta\delta_3$, ppm	
resonance	graphic extrapolation	computer regression	graphic extrapolation	computer regression
C_2	1.14	1.15	1.76	1.73
C_4	2.06	2.18	2.83	2.58
C_5	1.44	1.49	2.12	1.96
C_6	1.31	1.12	1.92	1.78
C_8	1.05	1.38	1.59	1.59
H_2	0.67	0.68	1.24	1.20
H_6	0.77	0.77	1.46	1.43
H_8	0.46	0.52	1.00	1.05

on a linear least-squares fitting method. At a given concentration, eq 1 can be rewritten in a general form:

$$\delta_{obsd} = \sum_{i=1}^{n} F_i\delta_i + \left(1 - \sum_{i=1}^{n} F_i\right)\delta_{rem} \qquad (2)$$

where F_i and δ_i are the mole fraction and chemical shift of the ith mer. δ_{rem} is the average chemical shift of the aggregate forms which have more units than the nth mer. Then eq 2 can be rearranged to

$$\delta_{obsd} = \sum_{i=1}^{n} F_i(\delta_i - \delta_{rem}) + \delta_{rem} \qquad (3)$$

When various concentrations of purine samples (from 1 to m) are considered together, eq 3 can be expanded to the following form:

$$\sum_{j=1}^{m} (\delta_{obsd})_j = \sum_{i=1}^{n}\sum_{j=1}^{m} F_{ij}(\delta_i - \delta_{rem}) + \delta_{rem} \qquad (4)$$

Equation 4 can be analyzed by a linear regression model with least-squares fitting of δ_{obsd}'s by searching δ_{rem} and $\delta_i - \delta_{rem}$ if F_i values are known. Programs for this kind of analysis are readily available. The analysis is done by a DEC-10 computer in Johns Hopkins University with a program entitled RLSER. In adopting eq 4 in the present computation, $n = 2$, $m = 11$-20 (for ^{13}C and ^1H resonances, respectively, over a concentration range of 0.02-1.01 M for ^{13}C and 0.001-1.04 M for ^1H data), and $\delta_{rem} = \delta_3$. These numerical analyses were carried out at three sets of conditions: at full range of entire concentration, at lower range of concentration, and at higher range of concentration (Table II). Figure 9 shows the satisfactory agreement between the experimental data and the line drawn for the regression analyses. The values of δ_1 for all eight resonances are essentially identical as derived from these two separate methods, i.e., graphical extrapolation and computer regression analyses. As for δ_2, the values from the graphic procedure are much closer to those obtained by the regression analyses limited to the lower concentration range than those obtained from the full range of concentration. Therefore, $\Delta\delta_2$ values were calculated based only on the values obtained by the graphic procedure and by the regression analyses at lower concentration range (Table III). This approach is reasonable, since at the lower concentration range for the calculation of chemical shifts for the dimer the uncertainty about the contribution of the shift, values of trimer, and other aggregated forms is substantially reduced. Similarly, for δ_3, the values from the graphic procedure are much closer to those obtained by the regression analyses focused on the higher concentration range than those obtained from the full range of concentration. This result is not unexpected, since the graphic procedure is based upon an extrapolation to infinite concentration. Therefore, again the graphic data and the regression analyses results at higher concentration region were used for the computation of $\Delta\delta_3$ (Table III). The agreements on the δ_1, δ_2, and δ_3 values derived by two separate procedures, i.e., graphic and regression, indicate the validity of both approaches.

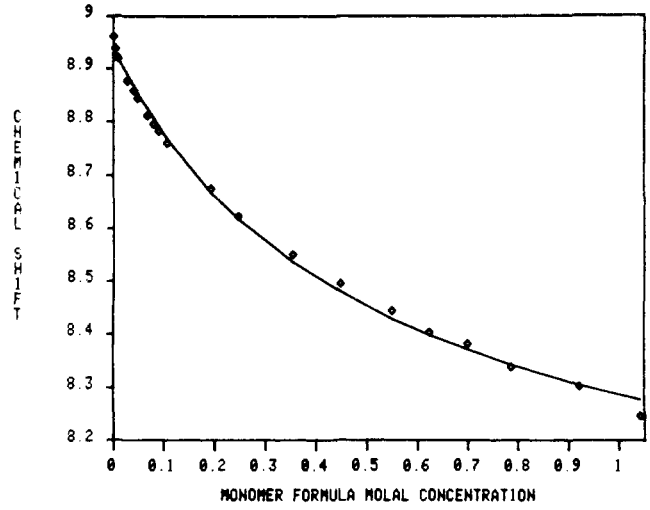

Figure 9. The experimental (◇) and computer-fitted (−) δ_{obsd} values of H_2 resonance vs. concentration of purine (0.001-1.04 M) at 25 °C.

Solvent Effect. In order to understand the possible solvent effect on nucleic acids, the following solvents are used: D_2O, dimethyl sulfoxide, pyridine, methanol, ethanol, and cyclohexane. In addition to purine, benzene and 1-butanol are examined for comparison; benzene represents ^1H and ^{13}C nuclei in an aromatic system and CH_3 of 1-butanol represents ^1H and ^{13}C nuclei in a saturated hydrocarbon. Unfortunately, purine

Table IV. δ_1 (ppm) Values of 1-Butanol (Methyl Group Only), Benzene, and Purine in Different Solvents at 25 °C (*p*-Dioxane Used as an External Standard)

compd	nuclei	solvents					
		D_2O	Me_2SO	pyridine	MeOH	EtOH	cyclohexane
1-butanol	C	53.72	51.79	54.11	53.93	53.74	53.76
	H	2.49	2.59	3.26	2.86	2.80	2.75
benzene	C	−61.88[a]	−61.80	−60.95	−60.45	−60.64	−60.55
	H	−4.04	−3.91	−3.19	−3.53	−3.60	−3.55
purine	C_2	−85.20[b]	−85.45[b]	−85.08[b]	−84.62[b]	−84.57[c]	
	C_4	−88.82	−88.24	−87.23	−87.58	−87.10	
	C_5	−61.88	−64.04	−65.08	−62.78	−63.08	
	C_6	−78.24	−78.95	−78.07	−77.62	−77.67	
	C_8	−80.85	−79.42	−79.15	−79.12	−78.64	
	H_2	−5.50	−5.47	−5.17	−5.15	−5.25	
	H_6	−5.67	−5.68	−5.26	−5.30	−5.45	
	H_8	−5.15	−5.18	−4.60	−4.77	−4.90	

[a] Trace amount. [b] Infinite dilution. [c] 0.09 M.

Table V. Solvent Shifts ($\Delta\delta^s$, ppm) of the Methyl Group of 1-Butanol, Benzene, and Purine in Five Solvents Referred to D_2O as Common Standard[a]

compd	nuclei	solvents				
		Me_2SO	pyridine	methanol	ethanol	cyclohexane
1-butanol	C	2.13[b]	−0.16	0.22	0.25	0.15
(methyl group only)	H	0.10	−0.54	0.06	−0.04	−0.07
benzene	C	0.12	−0.07	−1.00	−0.97	−1.14
	H	0.07	−0.62	−0.07	−0.17	−0.30
purine	C_2	0.45	0.11	−0.15	−0.36	
	C_4	−0.38	−1.36	−0.81	−1.45	
	C_5	2.36	3.43	1.33	1.47	
	C_6	0.91	0.06	−0.19	−0.30	
	C_8	−1.23	−1.47	−1.30	−1.94	
	H_2	0.17	−0.10	0.09	0.02	
	H_6	0.21	−0.18	0.07	0.05	
	H_8	0.23	−0.32	0.06	0.02	

[a] $\Delta\delta^s$ values have been corrected for bulk magnetic susceptibility with D_2O as a common basis for comparison (see text). [b] Negative values of $\Delta\delta^s$ denotes an upfield shift and positive values of $\Delta\delta^s$ denotes a downfield shift as compared to the resonance observed in D_2O.

does not dissolve in cyclohexane. Therefore, ^1H and ^{13}C spectra of purine in cyclohexane are not available. Table IV lists the chemical shifts of ^1H and ^{13}C resonances of the above compounds at infinite dilution, referring to their external standard, *p*-dioxane. For obtaining a solvent-independent δ value, a correction of bulk susceptibility may be made as follows:[22]

$$\delta^{S_1}{}_{corr} = \delta^{S_1}{}_{obsd} + \frac{2\pi}{3}(\chi_\nu{}^{ref} - \chi_\nu{}^{S_1}) \quad (5)$$

where $\delta^{S_1}{}_{obsd}$ is the observed δ in S_1 (see Table IV), $\chi_\nu{}^{ref}$ and $\chi_\nu{}^{S_1}$ are the bulk susceptibilities of the reference (*p*-dioxane) and solvent 1, and $\delta^{S_1}{}_{corr}$ is the correlated δ in solvent 1. For the sake of comparison to aqueous solution, the differences of chemical shifts in various solvents, $\Delta\delta^s$ or the solvent shifts, are referred to D_2O as a common basis instead of *p*-dioxane. Therefore

$$\Delta\delta^S = \delta^{D_2O}{}_{corr} - \delta^{S_1}{}_{corr} = \delta^{D_2O}{}_{obsd} - \delta^{S_1}{}_{obsd} + \frac{2\pi}{3}(\chi_\nu{}^{S_1} - \chi_\nu{}^{D_2O}) \quad (6)$$

The $\chi_\nu{}^{ref}$ is canceled since the same external reference (*p*-dioxane) is used in all measurements. In this convention, the negative value of $\Delta\delta^s$ denotes an upfield shift of the resonance of compound dissolved in solvent S_1 as compared to the resonance of compound dissolved in D_2O, while a positive value of $\Delta\delta^s$ would denote a downfield shift in the same comparison. These $\Delta\delta^s$ values at zero concentration by extrapolation are reported in Table V. It should be noted that the bulk susceptibility correction for ^1H ranges from +0.276 (D_2O) to −0.155 (methanol) and for ^{13}C from 0 (D_2O) to −0.188 (cyclohexane) and to −0.431 (methanol).

Discussion

A. Coupling Constants between ^{13}C and ^1H in Purine. The magnitudes of all possible ^{13}C-^1H coupling constants in purine have been unequivocally determined and listed in Table I. For one-bond coupling, magnitude roughly depends on the types of atoms next to the involved carbon. For example, in $^1J_{C2-H2}$ and $^1J_{C8-H8}$, each carbon has two nitrogen atoms as its nearest neighbors and larger coupling constants than $^1J_{C6-H6}$, in which C_6 has only one nitrogen atom in the neighborhood. This is because the nitrogen atom is more electronegative, thus increasing the value of $^1J_{C-H}$.[23]

Generally, the magnitude of three-bond carbon–proton coupling depends on its dihedral angle.[24] However, the purine molecule is planar.[25] Therefore, the dihedral angle effect on $^3J_{C-H}$ can be neglected. Thus, the magnitude of ^3J's is mainly determined by the electronic densities of the involved atoms.[26]

From Table I, it is clearly indicated that the values of $^3J_{C2-H6}$, $^3J_{C4-H2}$, $^3J_{C4-H8}$, $^3J_{C5-H8}$, and $^3J_{C6-H2}$ are larger than that of $^3J_{C4-H6}$, simply because in the former group there is a nitrogen atom in the covalent bond linkage, but not in $^3J_{C4-H6}$. The double-bonded character plays a minor role in *J* values and, as shown in Table I, the values of $^3J_{C2-H6}$, $^3J_{C4-H2}$, and $^3J_{C6-H2}$ are slightly larger than those of $^3J_{C4-H8}$. The former group has full double-bonded character while the latter one has a partial double bond.

Only one two-bond coupling exists in purine molecules. Therefore, there is insufficient experimental data from which to draw any conclusion. However, the magnitude of $^2J_{C5\text{-}H6}$ does not violate the previously drawn conclusions. There are two four-bond couplings in purine and their magnitudes are less than 1.5 Hz, similar to proton–proton coupling constants.[27]

B. Stacking Properties of Purine and Comparison between the Experimental Values of Chemical Shifts and Computed Values Based on Ring-Current Magnetic Anisotropy. The concentration dependence of ^1H chemical shifts of purine has been previously analyzed by Chan et al.[21] and by Cross.[8] This phenomenon has been correctly attributed to the vertical stacking of purine in aqueous solution. However, no quantitative comparison has yet been made between the observed upfield shifts and the through-space shielding effects due to ring current as well as local magnetic anisotropy. In this paper, an attempt is made for such a comparison for both ^1H and ^{13}C resonances. Qualitatively, the experimental $\Delta\delta_2$ values of C_4 and C_5, which are located at the middle of the base, are expected to be larger than those of C_2, C_6, and C_8, which are located at the peripheral of the base, which in turn are expected to be larger than those of protons H_2, H_6, and H_8. Indeed, these expectations are verified experimentally (Table V), indicating the general applicability of the ring-current magnetic anisotropy.

In a quantitative comparison between the experimentally determined dimerization shifts ($\Delta\delta_2$) and the computed dimerization shifts based on ring current as well as local magnetic anisotropy, the geometry of the purine bases in the stacks is an important consideration. Four approaches in formulating the geometrical models of the stacks have been adopted in a full exploration of this issue. First, a model based on maximal shielding of all the atoms on the average in the dimeric stack was constructed (Figure 10). Second, this all-atoms maximized model actually can have two modes, the parallel and the antiparallel stacks (Figure 10).

The coordinates of these models are described as follows. The point with the highest shielding in the purine molecule[2b] is defined as *M* (Figure 1). A straight line passing through this point and the atom C_8 is defined as the *X* axis. The *Y*-axis is in-plane and perpendicular to the *X* axis through point *M*. The *Z* axis is perpendicular to both *X* and *Y* axes through *M* and is assumed to be 3.2 Å, the distance between two base planes. The antiparallel model (Figure 10a) is constructed by rotating the second purine base 178° counterclockwise about the *Z* axis, with respect to the first base, so that the five-membered ring of the second base is on top of the six-membered ring of the first base. Then point *M* of the second purine is shifted with respect to point *M* of the first base by 0.58 Å along the *X* axis and by −0.03 Å along the *Y* axis.

The parallel model (Figure 10b) is constructed by rotating the second base 5° counterclockwise about the *Z* axis with respect to the first purine, so that the six-membered ring of the second base remains directly on top of the six-membered ring of the first base. Point *M* in the second base is then shifted by −0.10 and by −0.29 Å in *x* and *y* directions, respectively.

Third, we have also attempted to construct a model based on the maximal shielding of the C_4 atom (C_4 maximized model) since this atom is centrally located in the base. In addition, according to the all atoms maximized model, the difference between the experimental $\Delta\delta_2$ and the computed $\Delta\delta_2$ of C_4 atom is the largest among all atoms. Again, there are two modes in the C_4 maximized model, i.e., antiparallel and parallel modes. Finally, computation has also been made based on a mixture of dimer populations having two different geometries. In Table VII, the differences between the experimental $\Delta\delta_2$ and the computed $\Delta\delta_2$ are shown; the computed $\Delta\delta_2$ was based on a mixed population with 50% having a stacking mode of all-atoms-maximized model and 50% having a stacking model of C_4-maximized model.

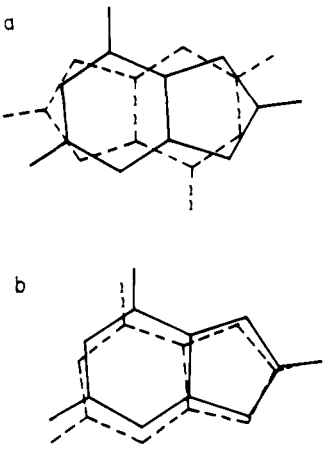

Figure 10. Stacking models of purines in a dimer constructed for maximal shielding of all atoms (all atoms maximized model): (a) antiparallel model; (b) parallel model.

The comparisons between the experimental $\Delta\delta_2$ and the computed $\Delta\delta_2$ for the eight atoms in the stack (Tables VI and VII) provide the following five conclusions: (1) The RC effect is larger than the LA contribution by approximately two- to fivefold. (2) Improved agreement between calculated and measured values is obtained when the RC and LA contributions are both taken into account in $\Delta\delta_2$ or $\Delta\delta_3$. An improvement of the calculated shifts when compared to the experimental ones has been previously obtained by addition of the LA contribution to the RC effect of intermolecular associations;[16,17] the present results tend to show that this phenomenon is quite general. (3) In general, the computed values are less shielded than the experimental values. (4) While the discrepancies vary among different atoms in different modes of stacking, the overall discrepancy as indicated by the mean value ($\bar{X}$) and standard deviation (*S*) was essentially the same, unaffected by the variation in the geometry of the stacks. This interesting finding implies that the general conclusion derived from the computation is unlikely to suffer from a systematic error or bias due to model building. In other words, reliable information can be obtained from this comparison, which is a test for the applicability and the adequacy of the ring-current plus atomic or local magnetic anisotropy theory as a basis for calculating the through-space shielding effects for both ^1H and ^{13}C resonances. This finding also suggests that, while it is likely that the two purines are held together in the dimer in close proximity with maximal contact, the mode of stacking is not dominated by a given form. This interpretation is in accord with the theoretical prediction in comparing the relatively low free energy of dimer formation ($K \approx 2.1$, $\Delta F = -440$ cal)[28] with thermal energy. (5) On the average, the agreement between the experimental and the computed $\Delta\delta_2$ is very satisfactory (mean variation ≈0.1 ppm with standard deviation ≈0.2 ppm). This degree of agreement may indeed exceed our expectation, based on the uncertainty of various factors. For instance, the current calculation is very sensitive to the parameter *Z*, the distance between the two purine bases in the stack. A change of 0.1 Å (a change from 3.2 to 3.3 or 3.1 Å) in this parameter will immediately bring about at least 0.2-ppm variation in the computed values. Among all the ^{13}C resonances, special attention should be focused on those from C_4 and C_5. In all the models studied, the calculated shielding is too small for the $^{13}C_4$ resonance with the difference, experimental $\Delta\delta_2$ − computed $\Delta\delta_2$, being largest for this atom, while on the contrary the value of this difference for the $^{13}C_5$ resonance is negative (Tables VI and VII). As described below,

Table VI. Dimerization Shifts, $\Delta\delta_2$, of Purines. Comparison between the Experimental and Computed Values Based on All-Atoms Maximized Model Z = 3.2 Å (Figure 10)

	computed $\Delta\delta_2$, ppm						exptl $\Delta\delta_2$ − total computed $\Delta\delta_2$[c]			
	antiparallel model[a]			parallel model[b]			antiparallel model		parallel model	
	ring current contribution	local magnetic anisotropies	total	ring current contribution	local magnetic anisotropies	total	graphic extrapolation	computer regression	graphic extrapolation	computer regression
C_2	0.72	0.27	0.99	0.93	0.25	1.18	0.15	0.16	−0.04	−0.03
C_4	1.42	0.34	1.76	1.34	0.31	1.65	0.30	0.42	0.41	0.53
C_5	1.46	0.32	1.78	1.35	0.33	1.68	−0.34	−0.29	−0.24	−0.19
C_6	0.86	0.27	1.13	1.01	0.27	1.28	0.18	−0.01	0.03	−0.16
C_8	0.86	0.26	1.12	0.65	0.25	0.90	−0.07	0.26	0.15	0.48
H_2	0.29	0.16	0.45	0.40	0.16	0.56	0.22	0.23	0.11	0.12
H_6	0.39	0.15	0.54	0.47	0.17	0.64	0.23	0.23	0.13	0.13
H_8	0.35	0.16	0.51	0.26	0.15	0.41	−0.05	0.01	0.05	0.11
$\bar{X}$[d]							0.08	0.13	0.08	0.12
S[e]							0.21	0.22	0.18	0.27

[a] Antiparallel model = two purine bases are stacked in such a manner that the five-membered ring of the second base is on top of the six-membered ring of the first base (Figure 10a). [b] Parallel model = the straight stacking with five-membered ring of the second purine directly above the five-membered ring of the first base (Figure 10b). [c] Positive values denote shielding while negative values denote deshielding. [d] $\bar{X}$ = mean = $1/n \sum_{i=1}^{n} x_i$. [e] S = standard deviation = $[(\sum_{i=1}^{n} (x_i - \bar{x})^2)/(n-1)]^{1/2}$ where $\bar{x}$ is the mean.

Table VII. Comparisons between the Experimental and Computed $\Delta\delta_2$ Based on C_4 Maximized Model at a Distance of 3.2 Å between Purine Planes (Z = 3.2 Å). Comparison Based on Equal Mixture of Population from C_4 Maximized Stacks and from All-Atoms Maximized Stacks (Table VI)

		computed $\Delta\delta_2$				exptl $\Delta\delta_2$ − computed $\Delta\delta_2$[a]			
		antiparallel model[a]		parallel model[a]		antiparallel model		parallel model	
	exptl $\Delta\delta_2$	C_4 max 100% pop.[b]	C_4 max. 50% pop.[c]	C_4 max 100% pop.	C_4 max 50% pop.	C_4 max 100% pop.	C_4 max 50% pop.	C_4 max 100% pop.	C_4 max 50% pop.
C_2	1.14	1.08	1.04	0.78	0.98	0.06	0.10	0.36	0.16
C_4	2.06	1.95	1.86	1.75	1.70	0.11	0.20	0.31	0.36
C_5	1.44	1.39	1.59	1.78	1.73	0.05	−0.15	−0.34	−0.29
C_6	1.31	0.74	0.94	1.30	1.29	0.57	0.37	0.01	0.02
C_8	1.05	1.03	1.08	0.94	0.92	0.02	−0.03	0.11	0.13
H_2	0.67	0.56	0.51	0.28	0.42	0.11	0.16	0.39	0.25
H_6	0.77	0.27	0.41	0.80	0.72	0.50	0.36	−0.03	0.05
H_8	0.46	0.47	0.49	0.42	0.42	−0.01	−0.03	0.04	0.04
$\bar{X}$[a]						0.18	0.12	0.11	0.09
S[a]						0.23	0.19	0.24	0.19

[a] See Table VI. [b] Ring-current contribution + local magnetic anisotropies. [c] 50% population of C_4 atom maximized model +50% population of all-atoms-maximized model (Figure 10).

Table VIII. Trimerization Shifts, $\Delta\delta_3$, of Purines. Comparison between the Experimental and Computed Values Based on All-Atoms Maximized Model Z = 3.2 Å (Figure 10)

	computed $\Delta\delta_3$, ppm						exptl $\Delta\delta_3$ − total computed $\Delta\delta_3$[a]			
	antiparallel model[a]			parallel model[a]			antiparallel model		parallel model	
	ring current contribution	local magnetic anisotropies	total	ring current contribution	local magnetic anisotropies	total	graphic extrapolation	computer regression	graphic extrapolation	computer regression
C_2	1.09	0.41	1.50	1.36	0.39	1.75	0.26	0.23	0.01	−0.02
C_4	2.05	0.50	2.55	1.95	0.48	2.43	0.28	0.03	0.40	0.15
C_5	2.10	0.48	2.58	1.95	0.54	2.49	−0.46	−0.62	−0.37	−0.53
C_6	1.29	0.40	1.69	1.49	0.42	1.91	0.23	0.09	0.01	−0.13
C_8	1.26	0.39	1.65	1.00	0.39	1.39	−0.06	−0.06	0.20	0.20
H_2	0.49	0.24	0.73	0.62	0.24	0.86	0.51	0.47	0.38	0.34
H_6	0.63	0.24	0.87	0.74	0.28	1.02	0.59	0.56	0.44	0.41
H_8	0.55	0.25	0.80	0.43	0.25	0.68	0.20	0.25	0.32	0.37
$\bar{X}$[a]							0.19	0.12	0.17	0.10
S[a]							0.33	0.37	0.28	0.32

[a] See Table VI.

these phenomena are probably related to the solvent effects and the tautomeric shift of the purines in the stack.

This same approach is extended to the comparison between the experimental and the computed trimerization shifts, $\Delta\delta_3$, based on the all atoms maximized model (Figure 10). Again, most of the computed values are smaller (mean variation ≈0.2 ppm) than those obtained experimentally; however, the $^{13}C_5$ resonance gives the largest discrepancy (Table VIII). It should be noticed that the LA contribution in the case of the trimer is proportionally smaller than the LA contribution in the case of the dimer.

C. **Solvent Effects.** The solvent shifts, $\Delta\delta^s$, of ^1H and ^{13}C nuclei in the methyl group of 1-butanol, benzene, and purine in five organic solvents as compared to D_2O are listed in Table

IV. Methanol/ethanol/cyclohexane represent a hydrocarbon-hydrophobic environment with special attention given to the comparison between the solvent effect in cyclohexane (a totally inert hydrocarbon) and that in methanol/ethanol, since purine can only be dissolved in the alcohols but not in cyclohexane. Pyridine and Me_2SO both have a lone pair of electrons for interaction and magnetic anisotropic effects, and in addition pyridine exerts a ring-current magnetic anisotropic effect, being an aromatic molecule. As for the two model compounds, the methyl group of 1-butanol provides a representative of alkane protons linked to a sp^3 carbon in a saturated hydrocarbon and benzene provides a representation of an aromatic proton linked to a sp^2 carbon in a resonant ring system.

The first interesting observation is that the solvent effects on the proton chemical shifts for the two model compounds and for purine are relatively small (~0.1 ppm), except in pyridine. In pyridine, owing to the ring-current effects of this aromatic solvent, the protons from both model compounds are shielded by about 0.6 ppm, though the pyridine effect on the purine protons is much smaller. It is likely that the shielding effects of the ring current of pyridine on purine are counteracted to a large extent by other interactions of the pyridine with the purine molecules. This is a comforting confirmation of the implicit assumption usually adopted in the calculation of the proton chemical shifts[3] that the solvent effects in processes of stacking-destacking (or helix-coil transition) can be neglected.

The situation of solvent effects for ^{13}C resonances is quite different and complicated. For the alkane, sp^3 carbon the transfer from D_2O to alcohol/hydrocarbon environment appears to have only a slight deshielding effect (~0.2 ppm), while for the aromatic, sp^2 carbon such a transfer appears to have a large shielding effect of about 1 ppm. More interestingly, the solvent effect of methanol/ethanol is the same as that of cyclohexane for these two model compounds. This observation indicates that for this study the environment in methanol/ethanol can be adopted as a useful approximation for a hydrocarbon-hydrophobic environment, usually represented by cyclohexane. As for the solvent effects of pyridine, it appears that the shielding effects observed in this solvent for the ^1H resonance of these two model compounds have been counteracted by a certain, unknown deshielding influence in the ^{13}C resonance. In Me_2SO, a large deshielding effect is observed for the ^{13}C resonance of the alkane carbon upon transferring from D_2O while negligible effects are observed for the aromatic carbon, presumably due to various effects counteracting each other.

As for the solvent effects on the ^{13}C resonances of purine, attention will first be directed to the transfer from D_2O to methanol/ethanol, which serves as a representation of a hydrophobic environment. In this transfer, the most striking observation is the large and opposite shift on the resonance of C_4 ($\Delta\delta^s = -1.45$ in ethanol) and of C_5 ($\Delta\delta^s = 1.47$ in ethanol). We propose that this phenomenon is related to the $N_7H \rightleftharpoons N_9H$ tautomerism in purine, based on the following lines of reasoning.

(1) It is known that $N_7H \rightleftharpoons N_9H$ tautomerism has a large and opposing effect on the ^{13}C chemical shifts of C_4 and C_5. Chenon et al.[11] showed that the change of methyl substitution from N_7 to N_9 in monomethylated purine causes an upfield shift of 9 ppm for C_4, and reversely a downfield shift of ~8 ppm for C_5. Based on this comparative study and the measured C_4 and C_5 resonance in Me_2SO, they calculated the population of N_7H tautomer to be about 40%, in agreement with the theoretical estimation that these two tautomers have about the same degree of intrinsic stability.[29]

(2) This automatic change of purine in alcohols and its effects on C_4 and C_5 chemical shifts can be understood from theoretical considerations. The calculation of Pullman, Bergmann, and their associates[30] indicated that the dipole moments for N_7 and N_9H are 5.5–6.0 and 3.3–4.2 D, respectively. It is therefore expected that the transfer of purine from D_2O (a medium of high dielectric constant) to methanol/ethanol (a medium of low dielectric constant) would favor the tautomeric shift from N_7H to N_9H significantly. Also, the calculation of Pullman and Pullman[29] show that the tautomeric shift of N_7H to N_9H of purine causes a gain of π-electron density in C_4 and C_8 atoms and a loss of π-electron density in the C_5 atom. Since it has been observed that the chemical shifts of the base carbon of purine and pyrimidine nucleosides are related more or less linearly and positively with π electrons,[31] it would be expected from this consideration that the resonances of C_4 and C_8 would be shifted upfield and the resonance of C_5 would be shifted downfield upon a tautomeric change of N_7H to N_9H in purine, as observed. Chenon et al.[11] also reported a upfield shift of C_8 upon a change of N_7-methylation to N_9-methylation. It should be noted that these solvent effects on C_4, C_5, and C_8 occur also in Me_2SO and pyridine, though the explanation may be complicated by other interactions and considerations.

As for the solvent effects on resonances of C_2 and C_6 upon a transfer from D_2O to alcohols, the observed effects are slight (Table V). It is likely, however, that these small effects are the results of counteracting influences. For example, the tautomeric change for N_7H to N_9H of purine is expected to have a deshielding effect on C_6 with little or no influence on C_2. On the other hand, the transfer of aromatic carbon of benzene from D_2O to alcohols has a large shielding effect but not the transfer of the alkane carbon, and C_2 and C_6 should be intrinsically more similar to the aromatic carbon than to the alkane carbon. Also, hydrogen bonding of N_1, N_3, N_7, and N_9 in D_2O and other solvents is expected to have differential effects on these carbons as shown by the ^{13}C study of Iwahashi and Kyogoku[32] between the complementary base pairing of adenine moiety and uracil/thymine moieties in chloroform/carbon tetrachloride. The magnitude observed in their study, however, is not large (below 0.5 ppm).

D. Concluding Remarks. The assignments, the concentration dependence of chemical shifts in aqueous solution, and the solvent effects of all eight ^1H and ^{13}C resonances of purine have been carefully determined. An attempt was made to evaluate quantitatively the change of chemical shifts of these eight resonances when the monomeric purine form a stack of dimer or trimer in aqueous solution. These changes, i.e., the dimerization shift ($\Delta\delta_2$) and the trimerization shifts ($\Delta\delta_3$), are being interpreted from two considerations: (1) the through-space effects due to ring-current and local magnetic anisotropy exerted by the bases to each other in the stack; (2) the solvent effect due to the exclusion of the water molecules upon formation of vertical stacks. Various geometrical models of the stacks were considered in the computation of the ring-current and local magnetic anisotropy effects. It was found that the overall comparisons between the experimental $\Delta\delta_2$ and computed $\Delta\delta_2$ are essentially not affected by various modes of orientation of the base in the stack.

On the average, the agreement between the experimental and the computed dimerization shifts ($\Delta\delta_2$) for ^{13}C and ^1H resonances has a mean variation of about 0.1 ppm and a standard deviation of 0.2 ppm, and the agreement for the trimerizations ($\Delta\delta_3$) has a mean variation of about 0.2 ppm and a standard deviation of 0.3 ppm. Such agreement indicates that the through-space effects of ring-current and local magnetic anisotropy can be applied quantitatively to both ^{13}C and ^1H resonances. However, the comparison between the experimental and computed $\Delta\delta_2$ of C_4 and C_5 strongly suggests that there is a shift of population of N_7H tautomers to the N_9H tautomers in the stack. This is understandable from the viewpoint of a change of dielectric constant from D_2O medium

to the hydrophobic stack. A tautomeric change of N_7H to N_9H for the purine would cause an upfield shift of the C_4 resonance and a downfield shift of the C_5 resonance. Therefore, it is important to assign C_4 and C_5 resonances properly. It should be noted that under certain conditions the solvent effect, i.e., the transfer of nuclei from aqueous environment to hydrophobic environment, on ^{13}C NMR shift, particularly for sp^2 carbon, can be substantial. This effect should be kept in mind in the interpretation of ^{13}C NMR of nucleic acids.

Acknowledgment. This research was supported in part by Grant PCM 77 25226 from the National Science Foundation and by the National Institutes of Health (GM 166066-11). We wish to thank Dr. A. A. Bothner-By for several useful discussions and Mr. J. Kast as well, for aid in the computer programming.

References and Notes

(1) (a) The Johns Hopkins University. (b) Institut de Biologie Physico-Chimique.
(2) (a) Johnson, C. E., Jr.; Bovey, F. A. *J. Chem. Phys.* **1958,** *29,* 1012–1014. (b) Giessner-Prettre, C.; Pullman, B. *J. Theor. Biol.* **1970,** *27,* 87–95.
(3) Borer, P. N.; Kan, L. S.; Ts'o, P.O.P. *Biochemistry* **1975,** *14,* 4847–4863. Kan, L. S.; Borer, P. N.; Ts'o, P. O. P. *Ibid.* **1975,** *14,* 4864–4869.
(4) DuVernet, R.; Boekelheide, V. *Proc. Natl. Acad. Sci. U.S.A.* **1974,** *71,* 2961–2228.
(5) Ts'o, P. O. P.; Melvin, I. S.; Olson, A. C. *J. Am. Chem. Soc.* **1963,** *85,* 1289–1296.
(6) Ts'o, P. O. P.; Chan, S. I. *J. Am. Chem. Soc.* **1964,** *86,* 4176–4181.
(7) Schweizer, M. P.; Chan, S. I.; Helmkamp, G. K.; Ts'o, P. O. P. *J. Am. Chem. Soc.* **1964,** *86,* 696–700.
(8) Cross, B. Thesis, University Microfilm 75-6982, Ann Arbor, Mich., 1974.
(9) Pugmire, R. J.; Grant, D. M.; Rubins, R. K.; Rhodes, G. W. *J. Am. Chem. Soc.* **1965,** *87,* 2225–2228.
(10) Thorpe, M. C.; Coburn, W. C., Jr.; Montgomery, J. A. *J. Magn. Reson.* **1974,** *15,* 98–111.
(11) Chenon, M. T.; Pugmire, R. J.; Grant, D. M.; Panzica, R. P.; Townsend, L. B. *J. Am. Chem. Soc.* **1975,** *97,* 4636–4642.
(12) Fischer, P.; Lösch, G.; Schmidt, R. R. *Tetrahedron Lett.* **1978,** *17,* 1505–1508.
(13) Live, D. H.; Chan, S. I. *Org. Magn. Reson.* **1973,** *5,* 275–276.
(14) Mantsch, H. H.; Smith, I. C. P. *Can. J. Chem.* **1973,** *51,* 1384–1391.
(15) Giessner-Prettre, C.; Pullman, B. *Biochem. Biophys. Res. Commun.* **1976,** *70,* 578–581.
(16) Barfield, M.; Grant, D. M.; Ikenberry, D. *J. Am. Chem. Soc.* **1975,** *97,* 6956–6961.
(17) Vogler, H. *Tetrahedron Lett.* **1979,** 229–232.
(18) Giessner-Prettre, C.; Pullman, B. *C. R. Acad. Sci.* **1969,** *268,* 1115–1117.
(19) Giessner-Prettre, C.; Pullman, B. *C. R. Acad. Sci.* **1968,** *266,* 933–936.
(20) Chertkov, V. A.; Sergeyev, N. M. *J. Am. Chem. Soc.* **1977,** *99,* 6750–6751.
(21) Chan, S. I.; Schweizer, M. P.; Ts'o, P. O. P.; Helmkamp, G. K. *J. Am. Chem. Soc.* **1964,** *86,* 4182–4188.
(22) Live, D. H.; Chan, S. I. *Anal. Chem.* **1970,** *42,* 791–792.
(23) Ellis, P. D.; Ditchfield, R. In "Topics in Carbon-13 NMR Spectroscopy", Levy, G. C., Ed.; Wiley: New York, 1976; Vol. II, pp 433–476.
(24) Alderfer, J. L.; Ts'o, P. O. P. *Biochemistry* **1977,** *16,* 2410–2416.
(25) Voet, D.; Rich, A. *Prog. Nucleic Acids Res. Mol. Biol.* **1970,** *10,* 183–244.
(26) Barfield, M.; Grant, D. M. *Adv. Magn. Reson.* **1965,** *1,* 149–193.
(27) Bothner-by, A. A. *Adv. Magn. Reson.* **1965,** *1,* 195–316.
(28) Ts'o, P. O. P. In "Basic Principles in Nucleic Acid Chemistry", Ts'o, P. O. P., Ed.; Academic Press: New York, 1974; Vol. I, pp 453–584.
(29) Pullman, B.; Pullman, A. *Adv. Heterocycl. Chem.* **1971,** *13,* 77–159.
(30) Pullman, B. *Jerusalem Symp. Quantum Chem. Biochem.* **1970,** *2,* 292–300. Pullman, B.; Bergmann, E. D.; Weiler-Feilchenfeld, H.; Neiman, Z. *Int. J. Quantum Chem., Suppl.* **1969,** *3,* 103–111.
(31) Jones, A. J.; Winkley, M. W.; Grant, D. M.; Robins, R. K. *Proc. Natl. Acad. Sci. U.S.A.* **1970,** *65,* 27–30.
(32) Iwahashi, H.; Kyogoku, Y. *J. Am. Chem. Soc.* **1977,** *99,* 7761–7765.

Proton Magnetic Resonance of NADH in Water–Methanol Mixtures. Conformational Change and Behavior of Exchangeable Proton Resonances as a Function of Temperature

James Tropp and Alfred G. Redfield*

Contribution No. 1286 from the Graduate Department of Biochemistry, Brandeis University, Waltham, Massachusetts 02154. *Received April 2, 1979*

Abstract: The proton magnetic resonance spectrum of NADH (nicotinamide adenine dinucleotide, reduced form) was studied in H_2O-methanol mixtures over the temperature range 35 to −20 °C using long pulse Fourier transform methods to suppress the solvent resonances. Addition of methanol to 40% by volume disrupted the ring stacking of NADH at 20 °C. Lowering the temperature caused restacking; the stacking enthalpy was estimated to be −3.5 to −4.2 kcal/mol. In 40% methanol, the amide resonance of NADH broadened and split as temperature was lowered from 35 °C. This behavior indicated the expected hindered rotation of the amide, but the measured rotation rates were unusually large (680/s at 20 °C) and the maximum peak separation at low temperature was unusually small (0.28 ppm). Possible explanations of these anomalies are discussed, including the possibility of hindered rotation of the entire carboxamide group. Several new resonances, due to exchangeable protons, appeared in the region 1.0–1.5 ppm downfield of H_2O as temperature was lowered from 20 °C. These were assigned to the ribose hydroxyl protons of NADH.

We have studied the proton magnetic resonance spectrum of NADH in H_2O-methanol mixtures, using long pulse and analogue filtering techniques[1] to suppress the solvent resonances. Our motivation was twofold: to study the behavior of exchangeable proton resonances and the amide group of NADH, and to investigate the effects of organic cosolvent and temperature upon its solution conformation.

We shall present evidence that addition of methanol to solutions of NADH at room temperature disrupts the ring stacked conformation of NADH, as recently observed by Oppenheimer et al.,[2] while lowering the temperature reestablishes the stacking. We find that lowering temperature causes broadening and splitting of the amide resonance, which we tentatively attribute to a hindered rotation about the amide carbonyl–dihydronicotinamide ring C-3 bond. Finally, we report the appearance, at low temperature, of several new resonances, in the range 1.0–1.5 ppm downfield of H_2O, which we assign to the ribose hydroxyl protons of NADH. Apart from our interest in the spectrum and properties of NADH, certain aspects of the present work are of technical interest. These

0002-7863/80/1502-0534$01.00/0